ISSN 1063-7761, Journal of Experimental and Theoretical Physics, 2007, Vol. 104, No. 3, pp. 417–422. © Pleiades Publishing, Inc., 2007.
Original Russian Text © E.B. Postnikov, A.Yu. Loskutov, 2007, published in Zhurnal Éksperimental'noĭ i Teoreticheskoĭ Fiziki, 2007, Vol. 131, No. 3, pp. 466–471.

NUCLEI, PARTICLES, FIELDS, GRAVITATION, AND ASTROPHYSICS

Wavelet Analysis of Fine-Scale Structures in the Saturnian B and C Rings Using Data from the Cassini Spacecraft

E. B. Postnikov[a] and A. Yu. Loskutov[b]

[a] *Kursk State University, Kursk, 305000 Russia*
[b] *Moscow State University, Moscow, 119992 Russia*
e-mail: postnicov@mail.ru; loskutov@chaos.phys.msu.ru

Received September 20, 2006

Abstract—A continuous wavelet transform with a complex Morlet basis offers an effective method for the analysis of an instant variable periodicity in the spatially inhomogeneous matter density in the radial structure of Saturn's rings. An original algorithm that reduces the integral transform to solving a Cauchy problem for a partial differential equation is used for an analysis of the images of Saturn's B and C rings, which were obtained in the second half of 2004 from the Cassini spacecraft. This paper is a continuation of our preceding study of the fine-scale structure of Saturn's rings reported in Zh. Éksp. Teor. Fiz. **128**, 752 (2005) [JETP **101**, 646 (2005)].

PACS numbers: 96.30.Wr, 05.45.-a

DOI: 10.1134/S1063776107030065

1. INTRODUCTION

The structure of the main Saturnian rings (A, B, C), especially that revealed on a fine-scale level by the Voyager spacecraft mission at the beginning of 1980s, is an object of extensive investigation representing a dynamical many-body system (for a detailed analysis of the state-of-the-art prior to the appearance of new data from the Cassini spacecraft, see [1]).

Now it is commonly accepted [2] that some of the most typical large-scale structures (density wave trains) are caused by the resonance interaction with Saturnian satellites, including Lindblad resonances (related to the radial perturbations produced by a satellite moving in a gravitational field of a nonspherical body) and vertical resonances (corresponding to the motion of a perturbing body over an orbit inclined to the ring plane). These factors are especially important for the fine-scale structure of Saturn's A ring.

The fine-scale structure of Saturn's two other main rings, B and C, is still incompletely clear [1]. It was suggested (see review [3]) that the fine-scale wave structure might be related to quasi-hydrodynamic phenomena in a continuous self-gravitating medium (e.g., to the Jeans-type instability, viscous overstability, etc.). It was also pointed out that the characteristic critical wavelengths at which such instabilities are observed amount to 30–200 m for ring A, 7–30 m for ring B, and fall below 7 m for ring C. Under the conditions typical of ring B, detailed numerical simulations based on the Navier–Stokes equation with and without allowance for self-gravitation [4] predicted the existence of radial structures comprising either narrow peaks separated by 80- to 100-m-wide empty gaps (the result of viscous instability of self-gravitating liquid) or wave structures with a characteristic length of up to 200 m. The latter structures can result from a viscous overstability, which represents a secondary unstable regime separated from the primary viscous instability by a gap corresponding to viscosities ensuring stable homogeneous distributions of particle density.

Apparently, these (and the other like) results require the development of special methods for the effective spatial-periodic deconvolution of images of the radial structures of Saturn's main rings. Based on the data on Saturn's A ring obtained from the Voyager spacecraft mission, Spilker et al. [5] used a window Fourier transform that revealed about 40 resonance structures which were attributed to the influence of various Saturnian satellites. At the same time, the analysis [5] indicated a number of resonance regions in which the achieved resolution and the capabilities of the processing algorithm were unable to resolve any features in the ring matter density distribution. For ring B, Horn and Cuzzi [6] performed a frequency analysis of the wave structures using a window Fourier transform, and Thiessenhusen et al. [7] studied the manifestations of higher resonances on the background of stochastic effects.

Since 2004, new data acquired by the interplanetary Cassini spacecraft have become available, including high-resolution photographs of the Saturnian rings (see [8] for a preliminary report of the Cassini research project group). We believe that these data can be suc-

cessfully processed using the wavelet transform technique—a method of analysis that has been actively employed in the past two decades—which aids the window Fourier transform in providing better adaptation to the specific features of analyzed signals in both spatial and temporal (frequency) domains. The efficiency of the wavelet transform with a simple Morlet wavelet basis in solving this task was successfully demonstrated by our study of resonance structures in Saturn's A ring [10]. The wavelet transform was performed using a new algorithm that reduced the integral transform to solving a Cauchy problem for a system of partial differential equations with the initial conditions representing the distribution under consideration. This approach ensured a higher accuracy and better resolution in taking into account the local properties of the distribution density.

This study is a continuation of our previous analysis of the structure of the main Saturnian rings as revealed by the high-resolution photographs made in 2004 by the Cassini spacecraft, which have been processed by the new wavelet transform method. However, since the fine-scale structure of the brightness distribution in the images of Saturn's B and C rings exhibits a more irregular character compared to that of the A ring, it is expedient to use the exact Morlet basis for the wavelet transform calculations.

2. CALCULATION ALGORITHM FOR A WAVELET TRANSFORM WITH A MORLET BASIS

If a signal under consideration is irregular and contains, on the one hand, almost harmonic components of finite duration and a constant or slowly varying frequency and, on the other hand, separate outbursts, a multiscale representation may require variation of the parameters of the analyzing wavelet within broad limits. Therefore, it is important to ensure that the wavelet function $\psi(\xi)$ would represent an element of the functional basis [9]. This implies that the wavelet image $w(a, b)$ must ensure exact restoration of the initial function $f(t)$. In particular, in the case of the energy normalization condition

$$\int |\psi(\xi)|^2 d\xi = 1$$

it is necessary that the function $f(t)$ have the following form:

$$f(t) = \frac{1}{C_\psi}\int\int w(a, b)\psi^*\left(\frac{t-b}{a}\right)db\frac{da}{a^2},$$

where the asterisk denotes the complex conjugate.

This form satisfies the wavelet admissibility condition that can be expressed either via the Fourier image as

$$C_\psi = \int \frac{|\hat{\psi}^*(\omega)|^2}{\omega} d\omega < \infty,$$

or via a requirement imposed on the wavelet proper:

$$\int_{-\infty}^{\infty} \psi(\xi) d\xi = 0.$$

This condition allows the signal to be restored from its image upon the corresponding processing.

As can be readily checked, the Morlet wavelet basis used in our previous investigation [10] does not obey the above condition. However, if the basis frequency is sufficiently high ($\omega_0 \geq \pi$), the integral rather negligibly differs from zero. This circumstance was used for the investigation of signals characteristic of the particle density distribution in Saturn's A ring.

The orthonormalized Morlet basis function is as follows [11]:

$$\psi(\xi) = \frac{1}{\sqrt[4]{\pi}} \times \left[\exp(i\omega_0\xi) - \exp\left(-\frac{\omega_0^2}{2}\right)\right]\exp\left(-\frac{\xi^2}{2}\right), \quad (1)$$

where the energy normalization is used because this norm is calculated much simpler (due to the presence of a difference in square brackets) than the amplitude norm. The corresponding integral wavelet transform can be written as

$$w(a, b) = \frac{1}{\sqrt{a}}\int_{-\infty}^{\infty} f(t)\psi^*\left(\frac{t-b}{a}\right)dt. \quad (2)$$

It was shown [12] that, in contrast to the case of a wavelet transform with the amplitude normalization, the local behavior of the instant period in the given case is more conveniently analyzed using a variant of the wavelet transform modulus rescaled as $|w(a, b)|^2/a$. Then, the period T of a monochromatic signal is determined from the relation

$$\frac{T}{2\pi}\left(\frac{T\omega_0}{2\pi a} - 1\right) = \exp\left(-\frac{4\pi\omega_0 a}{T}\right).$$

Previously, it was shown [10] that the wavelet transform with an amplitude norm of $\exp(-\omega_0^2/2)$ can be found as a solution to the Cauchy problem for a system of differential equations of the following type:

$$\frac{\partial u}{\partial a} = a\frac{\partial^2 u}{\partial b^2} + \omega_0\frac{\partial v}{\partial b},$$
$$\frac{\partial v}{\partial a} = a\frac{\partial^2 v}{\partial b^2} - \omega_0\frac{\partial u}{\partial b}. \quad (3)$$

The initial conditions for the real, $u(a, b) = \mathrm{Re}\,w(a, b)$, and imaginary, $v(a, b) = \mathrm{Im}\,w(a, b)$, parts of the wavelet

image in selecting the appropriate norm values are represented by the analyzed function proper and zero. In the case of an exact basis (1), the transition to a limit as $a \longrightarrow 0$ leads to a derivative of the Dirac delta, rather than to the delta function proper, which makes impossible the use $f(b)$ for $w(0, b)$.

However, the condition of linearity with respect to components of the kernel of the integral transform with the Morlet basis allows separate calculation of the quantities

$$W^{(1)}(a, b) = \int_{-\infty}^{\infty} f(t) \frac{\exp\left[-\frac{1}{2}\left(\frac{t-b}{a} + i\omega_0\right)^2\right]}{\sqrt{2\pi a}} dt, \quad (4)$$

$$W^{(2)}(a, b) = \int_{-\infty}^{\infty} f(t) \frac{\exp\left[-\frac{1}{2}\left(\frac{t-b}{a}\right)^2\right]}{\sqrt{2\pi a}} dt,$$

which obey the equations

$$\frac{\partial W^{(1)}}{\partial a} = a\frac{\partial^2 W^{(1)}}{\partial b^2} - i\omega_0 \frac{\partial W^{(1)}}{\partial b}, \quad (5)$$

$$\frac{\partial W^{(2)}}{\partial a} = a\frac{\partial^2 W^{(2)}}{\partial b^2}. \quad (6)$$

In the limit as $a \longrightarrow 0$, the kernels of both transformations (4) become delta functions and, accordingly, the initial conditions to Eqs. (5) and (6) acquire the following form:

$$\mathrm{Re}W^{(1)}(0, b) = \mathrm{Re}W^{(2)}(0, b) = f(b),$$

$$\mathrm{Im}W^{(1)}(0, b) = \mathrm{Im}W^{(2)}(0, b) = 0.$$

The system of equations for the real and imaginary parts of $W^{(1)}$ is analogous to Eqs. (3). In the $W^{(2)}$ function, only the real part is nonzero that is described by Eq. (6). Then, the required wavelet transform (2) with the Morlet basis (1) is expressed via auxiliary functions as

$$w(a, b) = \sqrt[4]{4\pi a^2}(W^{(1)}(a, b) - W^{(2)}(a, b)) \times \exp\left(-\frac{\omega_0^2}{2}\right).$$

Below, we present the results of calculations performed using the above algorithm with the aid of standard functions of the solution of a system of parabolic differential equations written in MATLAB language. In view of a finite length of the processed signals, the Cauchy problem was replaced by a boundary value problem with the boundary conditions of the first kind, which were represented by the initial values of the signal at the terminal points.

3. WAVELET IMAGES OF THE STRUCTURES OF SATURN'S B AND C RINGS

The approach described above has been applied to analysis of the matter density distribution using photographs made by the Cassini spacecraft in the period from October to December 2004. A narrow radial band was selected on each image from the NASA/JPL/Space Science Institute collection: PIA06535 (1024 × 15 pixels, Fig. 1a) and PIA06543 (1024 × 17 pixels, Fig. 2a) for the B ring and PIA06537 (1024 × 15 pixels, Fig. 3a) for the C ring (the center of the image occurs at a distance of 75000 km from Saturn). Figures 1b–3b show the signals obtained by averaging over the sampling sequence, where darker regions correspond to greater values of the function. Figures 1c–3c show the wavelet transform moduli with a base frequency of π; in Fig. 3d, this frequency was 2π. Regions exhibiting obvious distortions due to the edge effects were removed from the images.

Figure 1 shows a central region of the B ring, and Fig. 2 presents the external edge of this ring, where a homogeneous dark region with a thin bright band inside is the Huygens gap.

Note that the wavelet images of both imaged sites contain rather extended regions displaying a wave structure with weakly varying periods. In particular, Fig. 1c shows that a region with dimensionless coordinates from 0.2 to 0.65 (which corresponds to about 2000 km in absolute units) features a smooth variation of the period from 0.083 to 0.044 (i.e., from about 380 to 200 km), so that the line of maximum is stepwise with three plateaus. This region is followed by a segment of the line of maximum corresponding to a period of 0.025 (115 km). Fine-scale structures with an ordered instant periodicity are practically absent: in addition to "wedges" corresponding to the points of sharp local brightness variations, this level of resolution reveals only a sloped resonance line in the vicinity of a point with $b = 0.4$. Such a "background" periodicity was previously also reported [6], but the proposed wavelet transform reveals a "ladder" character of variation of the instant period. A possible physical explanation of this behavior is provided by a resonance mechanism analogous to that generating long-period resonance waves in the A ring (on both sides of the Encke gap), which interact weakly with the strong short-wave resonances.

In the wavelet image presented in Fig. 2c, the horizontal region of the wavelet maximum corresponds to a large-scale wave with a period of 0.063 (290 km). The

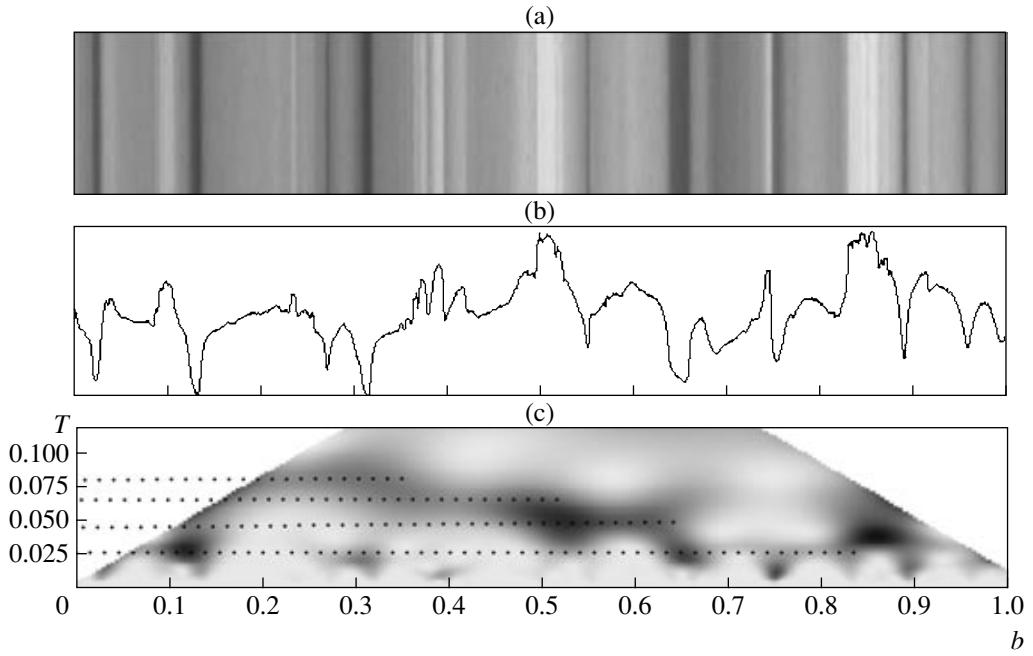

Fig. 1. Fine-scale structure of the central part of Saturn's B ring.

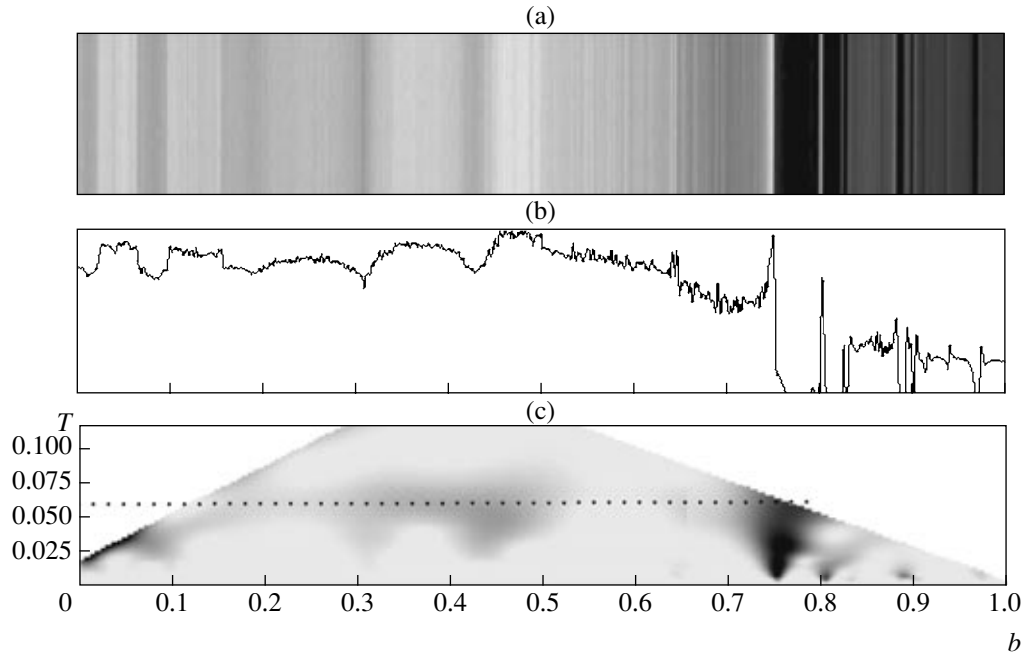

Fig. 2. Fine-scale structure at the external edge of Saturn's B ring.

corresponding perturbation is also clearly observed in the brightness distribution profile (Fig. 2b).

Figure 3 shows a region of the C ring, which exhibits a rich wave structure. In addition to the general background density wave with a period of 0.1 (460 km), this pattern clearly reveals two classical resonance curves. These resonances are also manifested in Fig. 3c, but they are most clearly pronounced in Fig. 3d, where the lines of maximum are emphasized by the black and white contrast lines. It should be noted that the appearance of a weak dark band situated below the white line is related to a large base frequency (leading to the manifestation of higher harmonics during the processing of

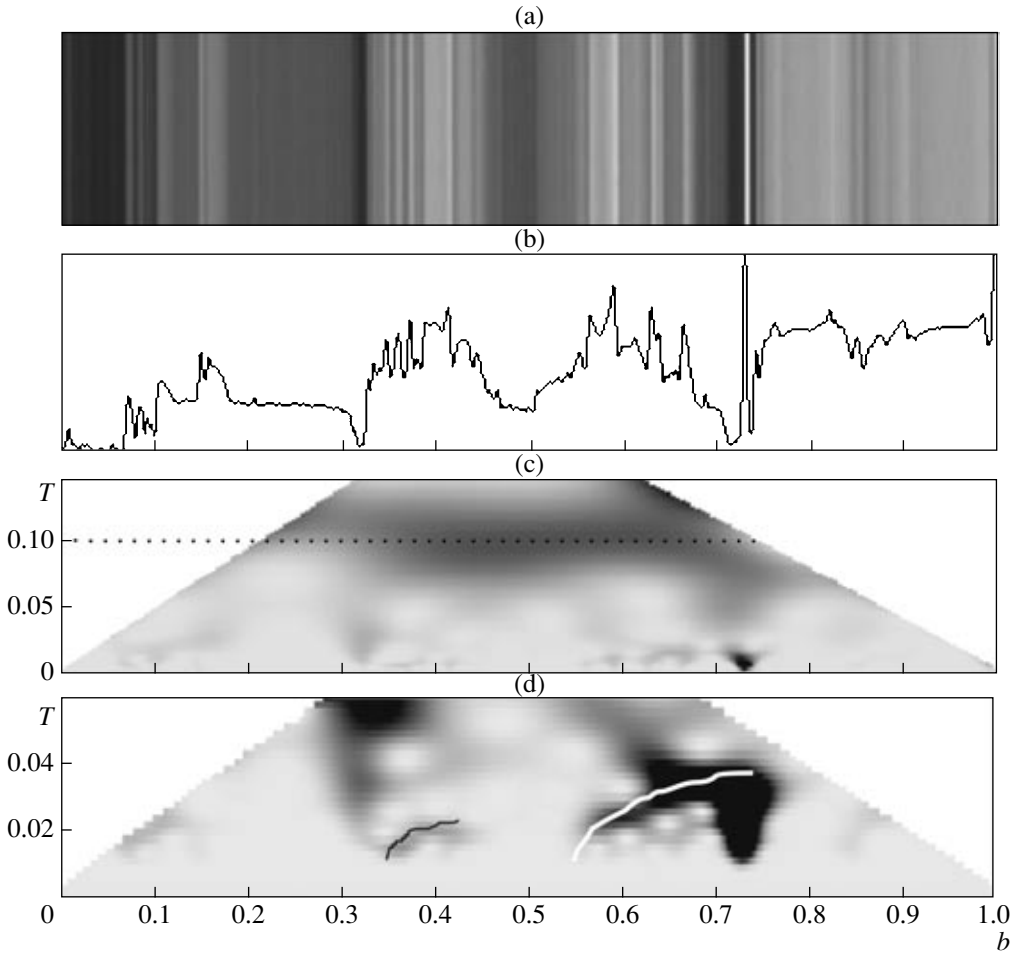

Fig. 3. Fine-scale structure of the central part of Saturn's C ring.

nonsinusoidal waves), rather than to the presence of an additional resonance.

4. CONCLUSIONS

The wavelet analysis of the structure of Saturn's B and C rings shows that these rings, as well as the A ring, exhibit wave perturbations on various scales, which weakly interact with each other. The character of the wavelet image confirms the relatively small fraction of resonance structures on the background of various short-wave outbursts. However, it was demonstrated in Section 2 that, in addition to the (previously reported) waves in ring B with stable spatial periods, there are long-wave resonance perturbations analogous to those generated by the shepherd satellites in the A ring.

It should be noted that, using the inverse wavelet transform for the exact form of the Morlet basis, it is possible to cut out, for example, all resonance trains from the radial signals. On the coordinate–period plane, such trains correspond to intense wavelet peaks forming a ladder pattern. Selecting the values of a wavelet image along the line of maximum and its small vicinity and substituting them into the relation for the inverse wavelet transform, it is possible to obtain a set of purely resonance oscillations. Then, subtracting them from the total signal, we obtain a plot of the function suited for the analysis of fine-scale structures. Localization of the regions of stable periodicity and determination of their periods in terms of the quasi-hydrodynamic model provides information about the density and composition of the Saturnian ring matter, which ensure the required intrinsic viscosity. The existence of a medium with this viscosity leads to the formation of a structure with the corresponding wavelength.

As can be readily seen, the complex wavelet transform is much better suited for the analysis of such systems than the other window transforms. These properties are related to the fact that, owing to self-similarity of the analyzing wavelet, the same characteristic number of oscillations cover the window in any frequency interval. Removal of the highest-frequency component (on scales close to zero) using the method described above makes it possible to cleanse the signal of the noise components (related both to the ring structure and to the instrumental noise). The separation of aperiodic

spots on the wavelet image makes possible the detection of structures comprising narrow dense ringlets.

REFERENCES

1. L. W. Esposito, Rep. Prog. Phys. **65**, 1741 (2002).
2. C. D. Murray, Lect. Notes Phys. **577**, 91 (2001).
3. E. Griv and M. Gedalin, Planet. Space Sci. **51**, 899 (2003).
4. U. Schmidt and W. M. Tscharnuter, Icarus **138**, 173 (1999).
5. L. J. Spilker, S. Pilorz, A. L. Lane, et al., Icarus **171**, 373 (2004).
6. L. J. Horn and J. N. Cuzzi, Icarus **119**, 285 (1996).
7. K.-U. Thiessenhusen, L. W. Esposito, J. Kurths, and F. Spahn, Icarus **113**, 206 (1995).
8. C. C. Porco, E. Baker, J. Barbara, et al., Science **307**, 1226 (2005).
9. S. Mallat, *A Wavelet Tour of Signal Processing* (Academic, New York, 1999).
10. E. B. Postnikov and A. Loskutov, Zh. Éksp. Teor. Fiz. **128**, 752 (2005) [JETP **101**, 646 (2005)].
11. I. Daubechies, *Ten Lectures on Wavelets* (SIAM, Philadelphia, 1992; RKhD, Izhevsk, 2004).
12. P. S. Addison, J. T. Watson, and T. Feng, J. Sound Vibr. **253**, 733 (2002).

Translated by P. Pozdeev